Finite Element Modeling of an Electrostatic Painting Device

G. Deliége, F. Henrotte, and K. Hameyer

***Abstract*—The system of coupled equations describing an electrostatic painting device is solved. The design of an efficient resolution strategy is discussed, and time integration schemes for the steady-state solution of the convection equation are compared.**

***Index Terms*—Convection, coupled problem, electrostatic painting, upwinding.**

I. Introduction

An electrostatic painting device is presented. Its behavior is modeled by a system of one static elliptic equation for the electric potential and three transient convection equations of the charge density due to ions, the concentration of particles, and the charge density due to painting particles, respectively. The convection equations require a particular treatment in order to avoid the oscillations resulting from an inadequate discretization of advective terms. These nonlinear relations are strongly coupled with each other.

In this paper, we leave out the introduction of painting particles and concentrate on the creation of ions at the cathode and their drift toward the anode. The system then reduces to one static elliptic equation and one transient convection equation. This approach allows us to determine the resolution strategy that could be applied to the complete system at a lesser computation cost. In particular, we discuss the choice of a time integration scheme able to compute the steady-state solution with a limited number of time steps but, nevertheless, with sufficient accuracy. We try to demonstrate that although the conservation of charge is satisfied only in a weak sense, our finite element formulation is perfectly suited for the resolution of the system as far as the space and time discretizations are sufficiently fine.

II. Description of the System

The device consists of a set of thin wires parallel to a grounded iron plate. The wires are brought to a high negative potential. The resulting electric field, particularly strong around the wires, causes the acceleration of free electrons that collide with neutral atoms [1]. If an electron has enough kinetic energy, the collision leads to the creation of a positive ion and a new electron that can in its turn interact with another atom. Free electrons are repelled by the cathode up to a point where the strength of the electric field is no longer sufficient to induce ionization. The electrons then combine with atoms to form negative ions that drift toward the anode, i.e. the grounded plate, due to Coulomb forces.

If coating particles are sprayed in the interval between the wires and the plate, which is filled with negative ions, they progressively acquire a negative charge and move toward the plate.

Manuscript received June 18, 2002; revised December 20, 2002. This work presents research results of the Belgian program on Inter-university Poles of Attraction initiated by the Belgian State, Prime Minister's Office, Science Policy Programming.

The authors are with Department ESAT, Division ELECTA, the Katholieke Universiteit Leuven, B-3000 Leuven, Belgium (e-mail: geoffrey.deliege@esat.kuleuven.ac.be).

Digital Object Identifier 10.1109/TMAG.2003.810210

III. Mathematical Model

A. Geometry

We limit the model to a box extending from the middle of a wire to half the distance between two consecutive wires (see Fig. 1). This model corresponds to a device with an infinite number of wires and does not take end effects into account. The main parameters of the system are given in Table I.

B. Equations

To obtain the distribution of ions and particles, the following system must be solved [2], [3]:

$$\nabla \cdot \mathbf{D} = \rho_i + \rho_q \tag{1}$$

$$\mathbf{D} = \varepsilon_0 \mathbf{E} \tag{2}$$

$$\mathbf{E} = -\nabla V \tag{3}$$

$$\partial_t \rho_i + \nabla \cdot (\rho_i \mathbf{v_i}) = -n_p \mathrm{D}_t q_p \tag{4}$$

$$\partial_t \rho_p + \nabla \cdot (n_p q_p \mathbf{v_p}) = n_p \mathrm{D}_t q_p \tag{5}$$

$$\partial_t n_p + \nabla \cdot (n_p \mathbf{v_p}) = 0 \tag{6}$$

along with [2]

$$\mathrm{D}_t q_p = \frac{\rho_i \mu_i Q_{\max}}{4\varepsilon_0} \left(1 - \frac{q_p}{Q_{\max}}\right)^2 \tag{7}$$

$$\mathbf{v_i} = -\mu_i \nabla V \tag{8}$$

$$\mathbf{v}_p = \frac{-q_p \nabla V + m_p \mathbf{g}}{6\pi\eta a} \tag{9}$$

where $\mathbf{v}_i$ and $\mathbf{v}_p$ are the ion and particle velocity, respectively, μ_i the ion mobility, η the viscosity of air, ρ_p the charge density due to the particles, n_p the particle concentration, and q_p, m_p, and a are, respectively, the charge, the mass, and the radius of one particle.

In [4], an analysis based on the comparison of one-dimensional solutions and experimental results yields an analytical expression of the flux of ions created around the cathode as a function of the electric field and the charge density. Thanks to this relation, the microscopic air ionization phenomenon, which occurs in a very thin region around the wire, is removed from the macroscopic model and replaced by a boundary condition.

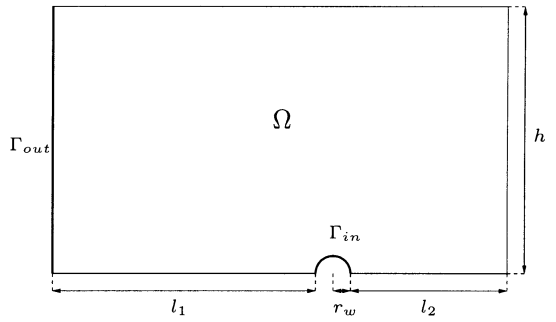

Fig. 1. Schematic representation of the geometry; Γ_{in} and Γ_{out} correspond to one half of a wire and the plate respectively.

TABLE I
PARAMETERS OF THE SYSTEM

parameter	value	unit
l_1	75	mm
l_2	50	mm
h	75	mm
r_w	0.05	mm
$V(\Gamma_{in})$	-35	kV
$V(\Gamma_{out})$	0	V
μ_i	$1.8\,10^{-4}$	V/s

IV. FINITE ELEMENT FORMULATION

In the absence of coating particles, ρ_p and n_p equal zero, and (1)–(9) reduce to

$$\nabla \cdot (\nabla V) = -\frac{\rho_i}{\varepsilon_0} \tag{10}$$

$$\partial_t \rho_i - \nabla \cdot (\mu_i \nabla V \rho_i) = 0 \tag{11}$$

in which a static elliptic equation is coupled to a transient convection equation. We solve (11) for ρ_i using a time integration scheme and update V thanks to (10) every time step or after a few steps if the variation of V is slow enough.

Equation (10) is easily solved with the finite element method. Its weak formulation is

$$\int_\Omega \nabla V' \cdot \nabla V d\Omega - \int_\Omega V' \frac{\rho_i}{\varepsilon_0} d\Omega = 0, \forall V' \in F_h^0(\Omega) \tag{12}$$

with

$$F_h^0(\Omega) = \left\{ V \in L^2(\Omega); \nabla V \in \mathbf{L}^2(\Omega), V|_{\Gamma_{in} \cup \Gamma_{out}} = 0 \right\}. \tag{13}$$

We fix V on the wire and the plate according to the values in Table I and set $\mathbf{E}_n = 0$ on the other boundaries.

The convection equation, on the other hand, must be handled more carefully. If the advective term is not discretised appropriately, serious accuracy problems might appear, leading in some cases to the appearance of nonphysical oscillations. Refining the mesh overcomes the problem at the cost of a higher number of unknowns. Upwinding techniques are an interesting alternative: The Galerkin formulation is replaced with, for instance, a streamline upwind Petrov–Galerkin (SUPG) formulation, leaving the number of unknowns constant [5].

Another difficulty comes from the fact that (11), which expresses the conservation of the electric charge, is satisfied only in a weak sense due to the finite element approach. The total electric charge of the system is thus not conserved, depending on the accuracy of the resolution. The error on the total charge will be used as a global error estimator and as a criterion to compare the accuracy of the time integration schemes.

A. Time Integration Scheme

It is well known that explicit time integration schemes are only conditionally stable when applied to convection equations, i.e., they are stable if the Courant number $C = (v\Delta t)/(h_e)$ does not exceed a constant depending on the scheme. The first-order explicit Euler scheme is unconditionally unstable, but the condition for the second order Lax–Wendroff scheme combined with first order finite elements is $C^2 \leq 1/3$. This condition can severely limit the time step Δt and, therefore, considerably increase the computation time. If C is evaluated in the vicinity of the wire, knowing the value of the electric field E and supposing that the circumference is discretized with at least 10 elements, we obtain $C \approx 10^8 \Delta t$. This forces us to make several thousands of iterations, even though we are interested only in the steady state.

Actually, it has been shown in [6] and [7] that Lax–Wendroff does not optimally combine with finite elements and that the third-order Taylor–Galerkin scheme gives more accurate results with a less severe condition ($C^2 \leq 1$) but at the cost of additional implicit terms in the mass matrix. Therefore, although Taylor–Galerkin provides very accurate solutions of transient problems, the limitation on Δt and the fact that the main advantage of explicit schemes is lost due to the consistent mass matrix make it ill suited for the computation of steady-state solutions.

In our case, it is thus preferable to use unconditionally stable schemes, such as implicit Euler or Crank–Nicolson. To obtain the corresponding formulations, we start from the Taylor expansion

$$\rho_i^{n+1} - \rho_i^n - \Delta t \left(\theta \partial_t \rho_i^{n+1} + (1-\theta) \partial_t \rho_i^n \right) = O(\Delta t^2) \tag{14}$$

and substitute the time derivatives of ρ_i thanks to (11). We premultiply by the SUPG weighting functions and integrate by parts to obtain the weak formulation

$$\begin{aligned}
&\int_\Omega \rho_i' \rho_i^{n+1} d\Omega - \int_\Omega \rho_i' \rho_i^n d\Omega \\
&- \Delta t \int_\Omega \nabla \rho_i' \cdot \mathbf{v} \left(\theta \rho_i^{n+1} + (1-\theta) \rho_i^n \right) d\Omega \\
&+ \Delta t \int_{\Gamma_{out}} \rho_i' \left(\theta \rho_i^{n+1} + (1-\theta) \rho_i^n \right) \mathbf{v} \cdot \mathbf{n} d\Gamma \\
&+ \Delta t \int_{\Gamma_{in}} \rho_i' J_n(\rho_i^n, \nabla V^n) d\Gamma \\
&+ \tau_e \int_\Omega \mathbf{v} \cdot \nabla \rho_i' \rho_i^{n+1} d\Omega - \tau_e \int_\Omega \mathbf{v} \cdot \nabla \rho_i' \rho_i^n d\Omega \\
&+ \Delta t \tau_e \int_\Omega (\nabla \rho_i' \cdot \mathbf{v}) \left(\theta \nabla \rho_i^{n+1} + (1-\theta) \nabla \rho_i^n \right) \cdot \mathbf{v} d\Omega \\
&+ \Delta t \tau_e \int_\Omega \rho_i' \nabla \cdot \mathbf{v} \left(\theta \nabla \rho_i^{n+1} + (1-\theta) \nabla \rho_i^n \right) \cdot \mathbf{v} d\Omega \\
&= 0, \quad \forall \rho_i' \in G_h^0(\Omega)
\end{aligned} \tag{15}$$

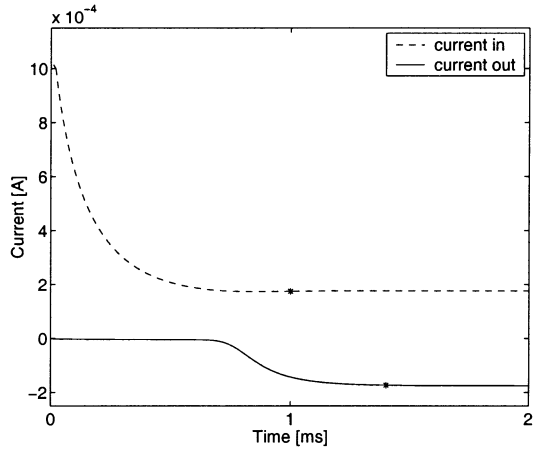

Fig. 2. Ion current flowing through the wire (in) and the plate (out); the "$*$" marks the point where the current has reached 99% of its steady-state value.

with

$$G_h^0(\Omega) = \left\{\rho_i \in L^2(\Omega); \nabla\rho_i \in \mathbf{L}^2(\Omega)\right\}. \tag{16}$$

Concerning the above formulation, we must add the following.

- τ_e is the SUPG parameter, depending on the characteristic size of the element h_e and the velocity $\mathbf{v}$ according to the formula

$$\tau_e = \frac{h_e}{2\|\mathbf{v}\|}. \tag{17}$$

  The formulation without upwinding is obtained by setting $\tau_e = 0$ in (15).
- The velocity $\mathbf{v}$ is equal to $(-\mu_i \nabla V^n)$. It is thus always computed with the electric potential at time step n, even when the time scheme is implicit. This simplification is justified by the fact that V varies much more slowly than ρ_i.
- The parameter $\theta \in [1/2, 1]$ determines the type of the scheme. The implicit Euler and Crank–Nicolson schemes, corresponding, respectively, to $\theta = 1$ and $\theta = 1/2$, are stable, whatever the time step.

However, the stability does not ensure the accuracy of the solution, which depends on the discretization of space and time. We are therefore going to investigate the influence of the time step and the mesh on the solution of (12)–(15) and make on basis thereof a comparison of the schemes corresponding to $\theta = 1$, $\theta = 1/2$, and an intermediate value $\theta = 2/3$. We pay particular attention to the conservation of the total charge. Let us define, therefore, the residual at time t^n

$$R_p(t^n) = \int_\Omega \rho_i^{n+1} - \rho_i^n d\Omega + \Delta t \int_\Gamma \rho_i^n \mathbf{v}^n \cdot \mathbf{n} d\Gamma \tag{18}$$

which quantifies the difference between the charge that has been gained or lost by the system through its boundaries during the time interval Δt and the effective variation of the total charge. We define the relative error r_ρ as the residual R_ρ divided by the total charge at steady state.

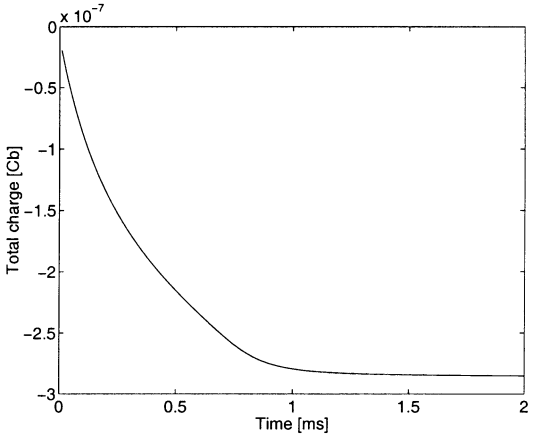

Fig. 3. Evolution of the total charge of the system.

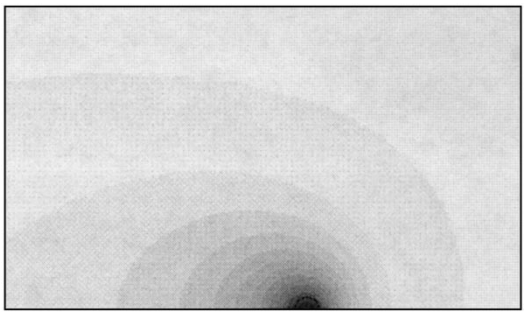

Fig. 4. Repartition of the charge density ρ_i at steady state, ranging from -510^{-4} Cb/m^3 (black) to 0 Cb/m^3 (white).

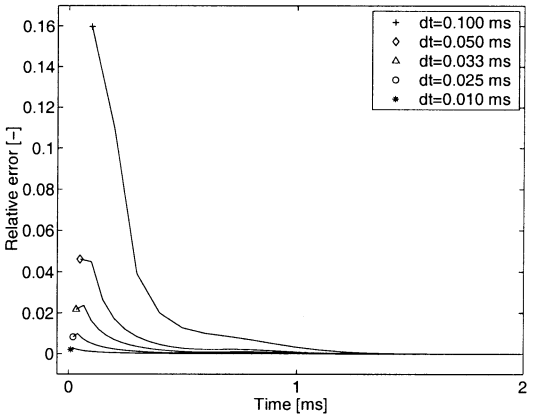

Fig. 5. Evolution of the relative error of the implicit Euler scheme ($\theta = 1$) when Δt ranges from 10 μs to 100 μs.

V. Results

A. Behavior of the System

We made a first series of computations in order to evaluate the characteristic time scale of the system as well as to outline its overall behavior. It appears that the ionization phenomenon reaches a steady state after 1 ms (see Fig. 2), and after 1.4 ms, the flux of ions reaching the plate compensates the flux of ions leaving the wire to within 1%. From that moment on, the total charge of the system must be constant, as confirmed by Fig. 3. The charge density ρ_i at $t = 2$ ms is drawn on Fig. 4. In view of

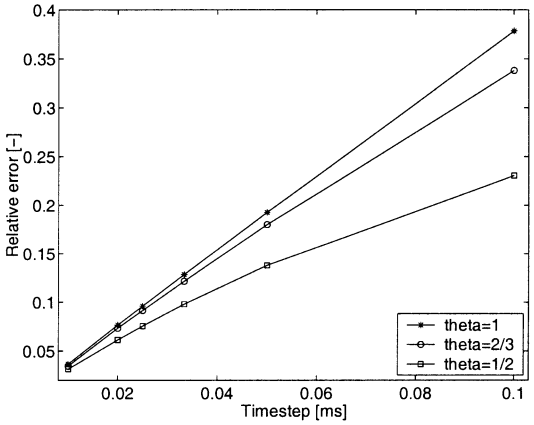

Fig. 6. Comparison of the relatives error of the time schemes.

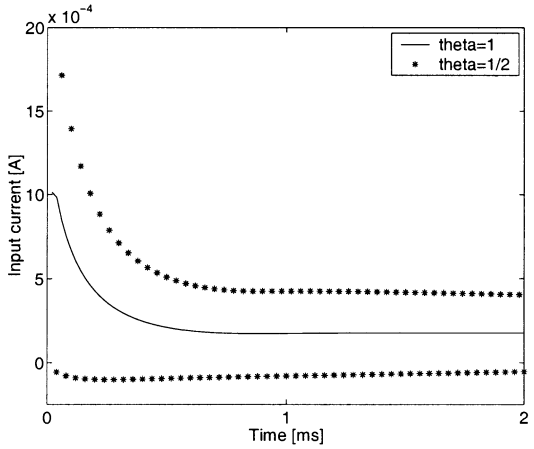

Fig. 7. Ion current through the wire for the Crank–Nicolson and the implicit schemes. The solution for $\theta = 1/2$ oscillates strongly around the exact solution.

these results, we have decided to perform all computations up to 2 ms.

B. Comparison of the Time Schemes

The dependence of the input current on the unknowns ρ_i and V does not induce strong linearities, and in accordance with our expectations, the first-order implicit scheme $(\theta = 1)$ is stable and converges to the same solution, whatever the time step. However, the influence of Δt on the conservation of charge is illustrated on Fig. 5, where the relative error r_ρ is plotted as a function of time. The error is maximum for the first steps and decreases regularly until steady state, where it is close to zero. Its maximum varies linearly with Δt, meaning we can easily bring it down to an arbitrary value by choosing the appropriate time step.

The comparison of the time schemes corresponding to $\theta = 1$, $\theta = 2/3$, and $\theta = 1/2$ is based on the same relative error integrated in time (see Fig. 6). From the point of view of charge conservation, the second-order Crank–Nicolson scheme seems to be more accurate than the other two. However, oscillations appear in the solution close to the wire when Crank–Nicolson is used and at a lower level with the $\theta = 2/3$ scheme (see Fig. 7). These oscillations remain bounded but propagate to the whole solution, even if they have little influence on the total output current and almost no influence at all on the evolution of the total charge. Actually, it has already been noticed in [6] that, in spite of its unconditional stability, the Crank–Nicolson scheme should not be used with a Courant–Friedrichs–Levy (CFL) number greater than one.

VI. Conclusions

An electrostatic painting device has been presented. Time integration schemes have been discussed, and implicit time schemes have been compared. It appears that the first-order implicit Euler scheme provides a solution free of oscillations and satisfactorily accurate: The error on the total charge related to the weak formulation of the conservation equation is easily controllable by an appropriate choice of the time step. The additional computation cost arising from the terms added in the mass matrix are compensated by the reduction of the number of steps by a factor of 100.

References

[1] C. Gary and M. Moreau, *L'effet de couronne en tension alternative*. Paris, France: Eyrolles, 1976.

[2] M. M. Pauthenier and M. Moreau-Hanot, "La charge des particules sphériques dans un champ ionisé," *J. Phys. Radium*, no. 7, pp. 590–613, May 1932.

[3] P. Lefèvre, F. Henrotte, W. Legros, and J. Schrynemackers, "Analysis of an electrostatic powder coating device," in *Proc. Int. Workshop Electric Magnetic Fields*, Ghent, Belgium, May 2000, p. 2.

[4] F. Henrotte, "Modélisation des efforts électromagnétiques et leurs effets dans les structures quelconques," Ph.D. dissertation, Univ. Liège, Liège, Belgium, Feb. 2000.

[5] A. N. Brooks and T. J. R. Hughes, "Streamline upwind Petrov–Galerkin formulations for convection dominated flows with particular emphasis on the incompressible Navier–Stokes equations," *Comput. Meth. Appl. Mech. Eng.*, vol. 32, pp. 199–259, 1982.

[6] J. Donea, L. Quartapelle, and V. Selmin, "An analysis of time discretization in the finite element solution of hyperbolic problems," *J. Comput. Phys.*, vol. 70, pp. 463–499, 1987.

[7] J. Donea, "A Taylor-Galerkin method for convective transport problems," *Int. J. Numerical Methods Eng.*, vol. 20, pp. 101–119, 1984.